Engineering Analysis with Boundary Elements 35 (2011) 244–252

Contents lists available at ScienceDirect

Engineering Analysis with Boundary Elements

journal homepage: www.elsevier.com/locate/enganabound

Shape variable radial basis function and its application in dual reciprocity boundary face method

Fenglin Zhou, Jianming Zhang*, Xiaomin Sheng, Guangyao Li

State Key Laboratory of Advanced Design and Manufacturing for Vehicle Body, College of Mechanical and Vehicle Engineering, Hunan University, Changsha 410082, China

ARTICLE INFO

Article history:
Received 9 February 2010
Accepted 11 June 2010
Available online 16 August 2010

Keywords:
Radial basis function
Dual reciprocity method
Boundary face method
Variable shape parameter
Poisson equation

ABSTRACT

The radial basis functions (RBFs) is an efficient tool in multivariate approximation, but it usually suffers from an ill-conditioned interpolation matrix when interpolation points are very dense or irregularly spaced. The RBFs with variable shape parameters can usually improve the interpolation matrix condition number. In this paper a new shape parameter variation scheme is implemented. Comparison studies with the constant shaped RBF on convergence and stability are made. Results show that under the same accuracy level, the interpolation matrix condition number by our scheme grows much slower than that of the constant shaped RBF interpolation matrix with increase in the number of interpolation points. As an application example, the dual reciprocity method equipped with the new RBF is combined with the boundary face method to solve boundary value problems governed by Poisson equations. Numerical results further demonstrate the robustness and better stability of the new RBF.

1. Introduction

The boundary element method (BEM) is an efficient alternative numerical technique for solving partial differential equations (PDE). For problems governed by Laplace equation, Helmholtz equation and linear diffusion-reaction equation, it has been widely used. In this method, the PDE is converted to an equivalent boundary integral equation (BIE) using Green's theorem and a fundamental solution. Thus, its main advantage over the classic domain methods, such as finite element method (FEM) and finite difference method (FDM), is the need of boundary only discretization together with a high rate of convergence. Nevertheless, when dealing with inhomogeneous problems, non-linear problems and more general linear PDEs for which fundamental solutions are unavailable or inconvenient, the BEM becomes less attractive since it is inevitable to discretize the considered domain for calculating the domain integrals that remain in the BIEs for the above problems.

To avoid the domain integrals, an alternative method named dual reciprocity method (DRM) was proposed by Nardini and Brebbia [1]. In this approach, the inhomogeneous term of the PDE is approximated by a series of simple functions and transformed to the boundary integrals employing particular solutions of considered problem. Since the accuracy and the stability of the solution depend largely on that of the approximation, the choice of the approximating functions in the series is usually of crucial importance in the DRM formulation. The most widely used approximating functions in DRM are radial basis functions (RBFs).

The RBF interpolation was pioneered by Hardy. After that there is a wide range of applications of the RBF, especially in meshless methods for solving partial differential equations [2,3]. Despite its simplicity and efficiency, the RBF interpolation suffers from a contradiction between accuracy and stability, which can be expressed in a form similar to the uncertainty principle in quantum mechanics [4]. The RBF interpolation matrix condition number becomes very large when the interpolation points are dense or irregularly spaced, and the ill-conditioned interpolation matrix limits its further application especially in large scale problems. To guarantee the robust of the interpolation many researchers have sought for the theoretical results about the convergence and stability of the RBF interpolation [4–8]. So far many methods have been proposed, such as compactly supported RBF, multilevel method, precondition method, domain decomposition method, truncated RBF method, RBF with variable shape parameter and knot optimization method [9]. The present paper focuses on the RBF with variable shape parameter.

The concept of variable shape parameters in the RBF interpolation has been proposed by many researchers, e.g. Kansa and Carlson [10]. The main idea is to determine the shape parameter of a RBF in terms of the local density of its corresponding interpolation point. Thus the columns of the interpolation matrix elements are more distinct, and the condition number becomes smaller. However, new problems may be caused by the shape parameter variation such as a singular interpolation matrix, lower convergence rate and difficulties to choose the variation schemes [11]. Many previous researches

* Corresponding author. Tel.: +86 0731 88823061.
E-mail address: zhangjianm@gmail.com (J. Zhang).

0955-7997/$ - see front matter © 2010 Elsevier Ltd. All rights reserved.
doi:10.1016/j.enganabound.2010.08.009

focus on solving problems caused by the shape parameter variation. Towards the singular interpolation matrix that may appear in the new interpolation method, Bozzini et al. [12] proposed some criterions for the shape parameter variation, which guarantee the unique solvability of the interpolation. Towards the variation schemes, Sarra and Sturgill [13] have verified a random variation scheme and Li et al. [14] have implemented a linear scheme successfully. Nevertheless, the variable shaped RBF was implemented to improve the accuracy rather than to improve the stability in the previous work. To the authors' knowledge, there is not yet any paper that implements this method with an emphasis on improving the stability of the interpolation. Whereas for engineering problems, the stability and the convergence of a method are often of more importance than its accuracy, because, generally speaking, the analytical solution for an engineering problem is usually unavailable. As the shape parameter variation scheme is the key factor in the successful implementation of variable shaped RBF interpolation, in this paper, we focus on the shape parameter variation scheme and proposed a quadric scheme for the variable shaped multiquadric (MQ) and a linear scheme for the variable shaped inverse MQ (IMQ) to improve the interpolation matrix condition numbers. Comparison studies showed that the variable shaped MQ with the proposed scheme outperformed the constant shaped MQ both on the accuracy and the stability, and that the variable shaped IMQ with the linear scheme outperformed the constant shaped IMQ on the stability. We also proposed a scheme for one of the variable shaped compactly supported RBF (CSRBF), but the comparison study showed that the improvement on the stability is not notable.

As an application example of the new RBFs, we also implement them in a combined approach of the DRM and the boundary face method (BFM) [15]. The BFM is an alternative approach for numerical solution of the BIE and implemented directly using the boundary representation (B-rep) data structure that is used in most CAD packages for geometry modeling. Both boundary integration and variable approximation are performed in the parametric space as in the hybrid boundary node method (HdBNM) [17–20]. The integrand quantities are calculated directly from boundary faces rather than from the standard elements as in the BEM, thus geometric errors can be avoided. When the BFM is implemented using shape functions from the moving least squares [16], it becomes a meshless method, and the BFM can be considered as a new implementation of the boundary node method (BNM) [21–22]. Recently, Qin and Zhang [23] have implemented the BFM using finite elements defined in the parametric space of boundary faces, which can be considered as a new implementation of the BEM. Our method is different from the boundary knot method [24] and the boundary particle method [25], which are simply some kind of collocation methods. In this paper, the BFM is combined with the DRM and facilitated by the variable shaped RBF to solve BVPs governed by Poisson equations. We call the combined method the dual reciprocity boundary face method (DRBFM).

The accuracy of the DRM mainly depends on two aspects: the method chosen to solve the BIE and the method for approximating particular solutions [15]. In the DRBFM, particular solutions are approximated by the variable shaped RBF, for which the error can be bounded by spectral norm of the inversed interpolation matrix. Hence, the condition number of the interpolation matrix can be controlled and better accuracy can be expected for the variable shaped RBF.

The paper is organized as follows. In Section 2 the RBF interpolation is given. Section 3 describes for the variable shaped RBF and shows comparisons on the stability and the convergence between constant shaped RBF and variable shaped ones. A brief description of the DRBFM and some numerical examples is given in Section 4. The paper ends with conclusions and discussions on future work in Section 5.

2. Outline of the RBF interpolation

2.1. Basic formulations

For given N data $f(x_i)=f_i$ for $i=1,2,\ldots,N$, where x_i's are N distinct points in R^d; the basis of the interpolation function was taken as

$$\varphi_j=\varphi(r_j)=\varphi(\|x-x_j\|) \quad j=1,2,\ldots,N \tag{1}$$

and all

$$p\in P_m^d \tag{2}$$

where m stands for the order of the positive definiteness [4] of the RBF and P_m^d denotes the space of d-variables polynomials of an order not exceeding m. The interpolation function is formed by

$$s_f(x)=\sum_{i=1}^{N}\alpha_i\varphi_i(x)+\sum_{j=1}^{M}\beta_j p_j(x) \tag{3}$$

in which M is the dimension of P_m^d. The coefficient vectors α and β can be determined by

$$s_f(x_i)=f_i \text{ for } i=1,2,\ldots,N \tag{4}$$

and

$$\sum_{j=1}^{N}\alpha_j p(x_j)=0 \text{ for all } p\in P_m^d \tag{5}$$

Actually the polynomials in the interpolation function are added to keep the equations uniquely solvable. The additional polynomials are not necessary if the RBF is strictly positive definite (SPD). In this paper, we focus on SPD RBFs.

2.2. Two categories of RBF

So far, many RBFs have been constructed, which can be sorted into two types: the globally supported RBF and the compactly supported RBF. Here we list some widely used globally supported RBFs:

Gaussians: $\exp\left(-\frac{r^2}{c^2}\right) \quad c>0$

Multiquadric: $(c^2+r^2)^{-\beta/2} \quad \beta\in R\backslash 2N, c\neq 0$

Thin-Plate Splines: $\begin{cases}(-1)^{1+\beta/2}r^{\beta}\log(r) & \beta\in 2N, \quad \text{even dimension}\\ r^{\beta} & \beta\in R_{>0}\backslash 2N, \quad \text{odd dimension}\end{cases}$

The Gaussian and the MQ are SPD RBFs, and the TPS is conditionally positive definite RBF of order 1. The global RBF often results in a dense and ill conditioned interpolation matrix. This poses high computational cost and serious stability problems. To avoid these drawbacks, compactly supported RBFs are getting popularity recently.

Compactly supported RBFs can be found in excellent works by Wu 26, Wendland 27 and Buhmann 28. Here we list Wendland's functions as follows:

$$\varphi_{l,0}(r)\doteq\left(1-\frac{r}{\delta}\right)_+^{l}$$

$$\varphi_{l,1}(r)\doteq\left(1-\frac{r}{\delta}\right)_+^{l+1}\left[(l+1)\frac{r}{\delta}+1\right]$$

$$\varphi_{l,2}(r)\doteq\left(1-\frac{r}{\delta}\right)_+^{l+2}\left[(l^2+4l+3)\left(\frac{r}{\delta}\right)^2+(3l+6)\frac{r}{\delta}+3\right]$$

$$\varphi_{l,3}(r) \doteq \left(1-\frac{r}{\delta}\right)_+^{l+3}\left[(l^3+9l^2+32l+5)\left(\frac{r}{\delta}\right)^3+(6l^2+36l+45)\left(\frac{r}{\delta}\right)^2+(15l+45)\frac{r}{\delta}+15\right]$$

where $l=[d/2]+k+1$, d denotes the dimensions, k stands for the order of the continuity of the functions and δ is the supporting scale of the CSRBF:

$$(1-x)_+ = \begin{cases} 1-x & x<1 \\ 0 & x\geq 1 \end{cases}$$

and $\doteq$ denotes equality up to a constant.

The implementation of the CSRBF in multivariate approximation usually leads to a sparse interpolation matrix. The supporting scale δ is the key importance to the stability and accuracy of the interpolation. However, it is still a challenge to find the best supporting scale of the CSRBF.

2.3. Error estimation and stability of the interpolation

The most famous error estimation and stability analysis of RBF interpolation were completed by Schaback [4]. Schaback's pointwise error estimation was given in the native space for the RBF. The formula is as follows:

$$|s_f(x)-f(x)| \leq |f|_N P(x) \tag{6}$$

where

$$|f|_N^2 = \int_{R^d} \frac{\left|\hat{f}(\omega)\right|^2}{\hat{\varphi}(\omega)} d\omega < \infty$$

and

$$N = \left\{ f \in L^2(R^n) \,\middle|\, \int_{R^d} \frac{\left|\hat{f}(\omega)\right|^2}{\hat{\varphi}(\omega)} d\omega < \infty \right\}$$

is called the native space of φ. The generalized Fourier transform is denoted by this. $P(x)$ is called the power function; it is bounded by $F(h(x))$, which has different representations for different RBFs. The shape parameters of the RBFs, however, are not directly contained in these representations. In that paper, the stability was given by a lower bound for the eigenvalue λ of the interpolation matrix, and the lower bound was denoted by $G(h(x))$; the exact forms of $F(h(x))$ and $G(h(x))$ for some kinds of global RBF can be found in table 1 in [2]. It is worth noting that in the formulation of $G(h(x))$ for the MQ and the Gaussian, the shape parameters of both RBFs are contained.

$$\text{For the MQ: } G(h) = h^{-1}e^{(-12.76cd/h)} \tag{7}$$

$$\text{For the IMQ: } G(h) = he^{(-12.76cd/h)} \tag{8}$$

$$\text{For the Gaussian: } G(h) = h^{-d}e^{(-40.71c^2d^2/h^2)} \tag{9}$$

where $h = \sup_{y\in\Omega}\min_{x\in X}\|x-y\|$, X is the set of all the interpolation points, d denotes the dimensions and c is the shape parameter of the corresponding RBF.

Wendland [8] estimated the relative errors for his CSRBF of minimal degree. The interpolation error estimation of the CSRBF of their minimal degree was given by

$$\|f-s_{f,X}\|_{L^\infty(\Omega)} \leq C\|f\|_{H^s(R^d)}\left(\frac{h}{\delta}\right)^{k+1/2} \tag{10}$$

where f is a function from $H^s(R^d)$, $s=d/2+k+1/2$, which coincides with the native space of $\varphi_{d,k}$. $h = \sup_{y\in\Omega}\min_{x\in X}\|x-y\|$ is called the fill distance, and C is a constant independent of the fill distance and the interpolated function. Moreover the condition number of the interpolation matrix was bounded above by

$$C_1\left(\frac{q}{\delta}\right)^{-d-2k-1} \tag{11}$$

where C_1 is some constant independent of $q = \min_{1\leq i<j\leq N}\|x_i-x_j\|$ [25]. $h \approx q/2$ is usually valid when the interpolation points are regularly distributed.

3. RBF with spatially variable shape parameters

3.1. Role of the shape parameter in RBF interpolation

The shape parameter of RBF is another important factor that affects the interpolation error and stability. For the MQ case, Huang et al. [29] had found that theoretically larger value of the shape parameter often results in high accuracy. Nevertheless, the condition number of the interpolation matrix is usually huge for large value of the shape parameter. An optimal (in the sense of the highest accuracy) value of the shape parameter of MQ was found in [29]. Similar phenomenon appears in Gaussian and IMQ cases. In CSRBF case, the support scale plays the same role as the shape parameter plays in the globally supported RBF case. The density of the interpolation matrix depends largely on the scale of the supporting domain. Large supporting scale often results in a high accuracy whereas the interpolation usually suffers from a dense and ill conditioned matrix.

3.2. The variable shaped RBF

Most literatures about the variable shaped RBF focus on improving the accuracy of the interpolation. To the authors' knowledge, there is not yet a paper emphasizing on improving the stability of the interpolation through the variable shaped RBF.

The variation scheme is a crucial importance to the performance of the variable shaped RBF. The variation scheme to improve the stability of the interpolation is different from that aiming to improve the accuracy of the interpolation. To improve the stability of the interpolation, the shape parameter of the RBF is determined according to the minimal distance between the corresponding interpolation point and its adjacent points. Thus the corresponding columns of the interpolation matrix are more distinct, and the condition number decreases. Although the accuracy becomes two or three orders magnitude less than the constant shaped RBF, the condition number can be well controlled. In constant shaped RBF case, a smaller value of the shape parameter can also lead to a better conditioned interpolation matrix. The condition number, however, grows too rapid to keep the stability of the interpolation with a decrease in interpolation error especially when the interpolation points are irregularly distributed. We propose variation schemes through which the interpolation matrix condition number grows slower than that of the constant shaped RBF with increase in interpolation points. We compare the constant shaped RBF and the variable shaped RBF on the convergence and the stability of the interpolation. Furthermore three kinds of RBF as follows are verified.

(i) MQ: $\varphi = \sqrt{r^2+c^2}$
(ii) Inverse MQ: $\varphi = 1/\sqrt{r^2+c^2}$
(iii) Wendland's $\varphi_{3,1}$: $\varphi = (1-(r/\delta))_+^4(4(r/\delta)+1)$

For the MQ, we are inspired by the upper bound of λ^{-1}, which is a representation of the interpolation sensitivity, and the bound is of the form:

$$\frac{1}{h}e^{(38.28c/h)} \text{ in 3D} \tag{12}$$

Two variation schemes are proposed for the MQ, they are

$$c_i = h_i^2 \tag{13}$$

and

$$c_i = 5h_i^2 \tag{14}$$

where $h_i = \min_{1 \le j \le n^3, j \ne i} \|y_i - y_j\|$, y_i denotes the ith interpolation point. In constant shaped RBF cases, we substitute Eq. (13) into expression (12), the new upper bound as follows is obtained:

$$\frac{1}{h}e^{38.28h} \tag{15}$$

We have $(1/h)e^{38.28h} = O(h^{-1})$ when h goes to zero. On the other hand, the error estimation for the MQ in [4] is given by an upper bound of the power function as introduced in Section 2:

$$P^2(x) \le F(h) = e^{-\frac{\sigma}{h}} \tag{16}$$

where σ is a constant independent of h, but it is usually a function of the shape parameter. A balance between the accuracy and the stability of the interpolation may be found through the quadric variation scheme (Eq. (13)).

For the IMQ, The bound of λ^{-1} is of the form:

$$\lambda^{-1} \le he^{(38.28c/h)} \tag{17}$$

We propose the variation scheme

$$c_i = 2.5h_i \tag{18}$$

for this RBF. If we substitute Eq. (18) into inequality (17), the new upper bound for the IMQ is obtained:

$$\lambda^{-1} \le 2.5he^{95.7} \tag{19}$$

We have $2.5he^{95.7} = O(h)$ when h goes to zero. On the other hand, Huang et al. [29] proposed the error estimation for the IMQ:

$$\varepsilon \sim O(e^{ac^{1.5}} \lambda^{c^{0.5}h^{-1}}) \tag{20}$$

where $a > 0$, $1 > \lambda > 0$ are real constants and ε denotes the interpolation error. A higher degree of h in Eq. (15) may lead a lower convergence rate, but it usually results in an interpolation matrix condition number with lower increasing rate. The balance between the accuracy and the stability of the IMQ interpolation may be found through the linear variation scheme (Eq. (18)).

When we turn to Wendland's twice continuously differentiable CSRBF $\varphi_{3,1}$, the interpolation matrix condition number has a bound of the form:

$$Cond(A) \le C_1 \left(\frac{h}{\delta}\right)^{-6} \tag{21}$$

where $Cond(A)$ stands for the condition number of the interpolation matrix A. We proposed the variation scheme:

$$\delta_i = 5h_i^{2/3} \tag{22}$$

for this CSRBF. Substituting Eq. (22) into inequality (21), the bound for the condition number becomes

$$Cond(A) \le C_2 h^{-2} \tag{23}$$

It is four orders lower than that in inequality (21). Nevertheless, when we substitute Eq. (22) into inequality (10), the new convergence rate is only one order lower than that in inequality (10).

Here we use a numerical example to verify the schemes above. In the example, the interpolation points are distributed in $\Omega = [-1,1] \times [-1,1] \times [-1,1]$ with coordinates given by

$$(x_1^i, x_2^j, x_3^k) = \left(-1 + 2 \times \left(\frac{i}{n}\right)^2, -1 + 2 \times \left(\frac{j}{n}\right)^2, -1 + 2 \times \left(\frac{k}{n}\right)^2\right) 1 \le i \le n, 1 \le j \le n, 1 \le k \le n,$$

where n denotes the number of the interpolation points in each direction. The interpolated function is given by

$$f = \sin(2x)\sin(2y)\cos(2z)$$

The condition number is defined as $Cond(A) = \|A\|_1 \|A^{-1}\|_1$, where

$$\|A\|_1 = \max_{1 \le j \le n} \sum_{i=1}^{n} |a_{ij}|$$

The parameter of the constant shaped RBF is evaluated with the average value of all variable parameters. The comparisons between constant shaped RBFs and variable ones are shown in Figs. 1–6.

Fig. 1 shows the convergence of the MQ interpolation using both variable and constant shape parameter. The convergence rate of both the constant shaped and the variable shaped MQ is nearly the same. The corresponding interpolation matrix condition number is presented in Fig. 2. The interpolation matrix condition number of the quadric schemed variable shaped MQ grows much slower than that of the constant shaped MQ with increase in interpolation points. It is demonstrated that the quadric variation scheme for the variable shaped MQ can improve the stability of the interpolation and that more accurate results can be obtained stably with adding interpolation points by this new method.

Figs. 3 and 4 show the comparisons between the variable shaped IMQ and the constant shaped IMQ on the convergence and the condition number of the interpolation matrix. Although the convergence rate is relatively low, the interpolation matrix condition number of the linear schemed variable shaped IMQ grows much slower than that of the constant shaped IMQ.

Figs. 5 and 6 show comparisons between the variable shaped $\varphi_{3,1}$ with the variation scheme (Eq. (22)) and the constant shaped $\varphi_{3,1}$ on the convergence and the interpolation matrix condition number. No notable improvement on the accuracy and the condition number appears in these comparisons. This can be explained by the fact that the span of the variable parameters (they are the supporting scales here) cannot be very large under

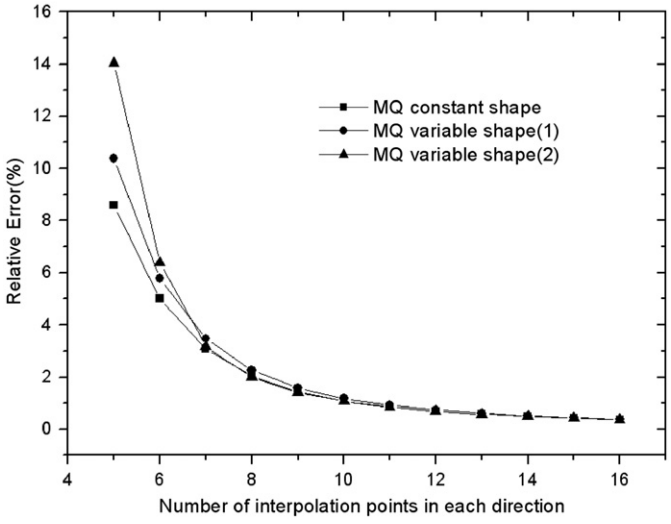

Fig. 1. Relative error versus the density of the interpolation points for the MQ.

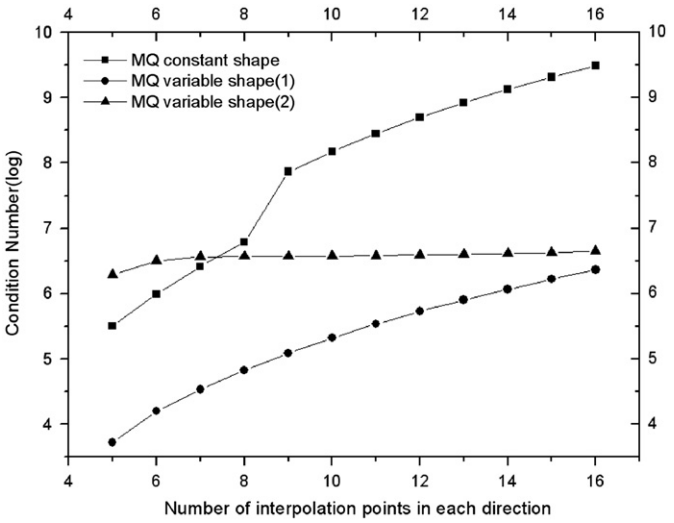

Fig. 2. Condition number versus the density of the interpolation points for the MQ.

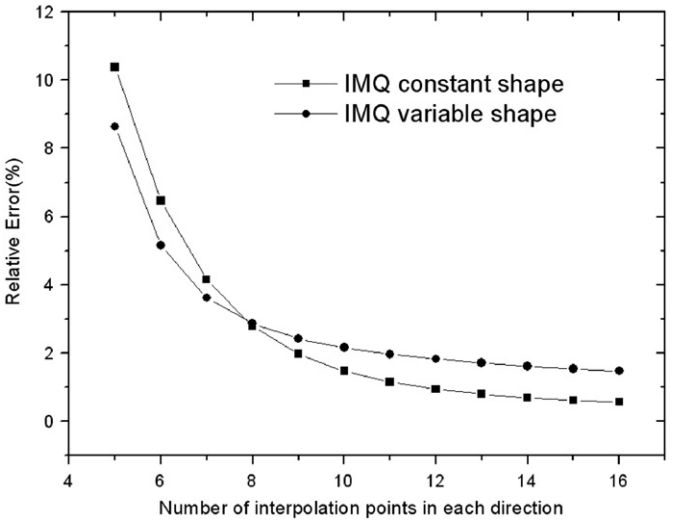

Fig. 3. Relative error versus the density of the interpolation points for the IMQ.

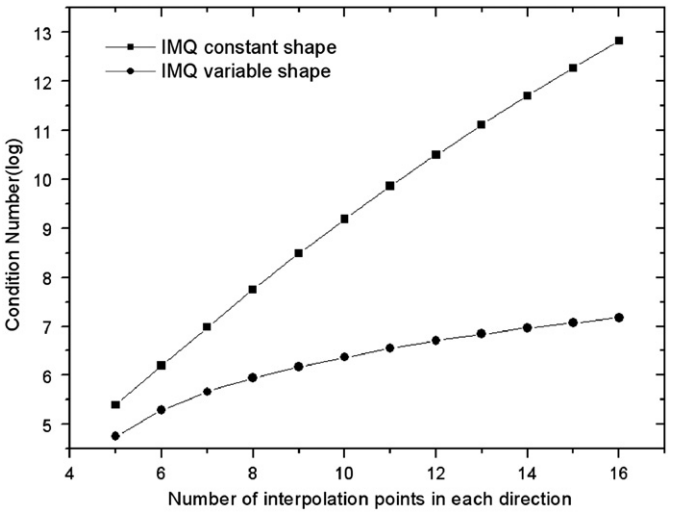

Fig. 4. Condition number versus the density of the interpolation points for the IMQ.

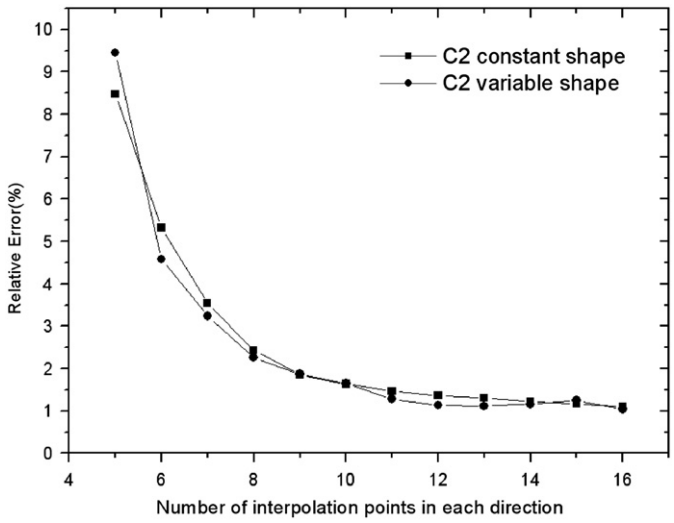

Fig. 5. Relative error versus the density of the interpolation points for $\phi_{3,1}$.

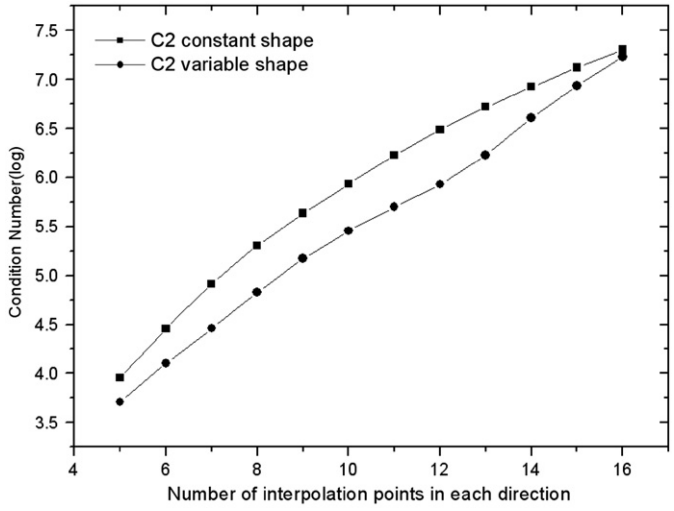

Fig. 6. Condition number versus the density of the interpolation points for $\phi_{3,1}$.

the chosen variation scheme. Both of the constant shaped CSRBF and the variable shaped one with the variation scheme (Eq. (22)), however, result in an acceptable condition number of the interpolation matrix.

All the comparisons showed that the stability of the globally supported RBF interpolation can be largely improved using properly schemed variable shape parameters, and the CSRBF with properly chosen scale can result in acceptable condition number increasing rate. We will apply variable shaped MQ with a quadric variation scheme in the DRBFM to improve the accuracy and the stability.

4. Dual reciprocity boundary face method

4.1. Description of the dual reciprocity boundary face method

In the conventional BEM, the geometry coordinates are approximated through the standard element, thus inevitably producing geometric errors. In the BFM, both the integration over the boundary and the variable approximation are performed in the parametric space. The integrand quantities such as the coordinates of Gauss integration points, Jacobian and out normal

are calculated directly from the faces, which are represented in parametric form, rather than from standard elements as in FEM and BEM, and thus geometric error can be avoided. In this paper we combine the BFM and the DRM together to solve boundary value problems governed by Poisson equations.

We consider a boundary value problem in potential theory:

$$\begin{cases} \nabla^2 u = b, & \forall x \in \Omega \\ u = \overline{u}, & \forall x \in \Gamma_u \\ \dfrac{\partial u}{\partial n} \equiv q = \overline{q}, & \forall x \in \Gamma_q \end{cases} \tag{23}$$

where the domain Ω is enclosed by $\Gamma = \Gamma_u \cup \Gamma_q$, $b=b(x,y,z)$ is the distribution of the heat source, and $\overline{u}$ and $\overline{q}$ denote for the known potential and normal flux on the essential boundary Γ_u and on the flux boundary Γ_q, respectively.

In the DRM, the inhomogeneous term is approximated by a series of RBFs:

$$b \approx \sum_{i=1}^{N+L} \alpha_i \varphi_i \tag{24}$$

where N and L are the number of boundary points and inner points, respectively. $\alpha = \{\alpha_1, \alpha_2, \ldots, \alpha_{N+L}\}$ is the coefficient vector, which can be determined by the following equation:

$$F\alpha = b \tag{25}$$

where F is the interpolation matrix of order $N+L$ and the entries of vector b are values of the interpolated function at each point. Substituting Eq. (24) into the governing equation, we have

$$\nabla^2 u = \sum_{i=1}^{N+L} \alpha_i (\nabla^2 \phi_i) \tag{26}$$

ϕ_i, which satisfies $\nabla^2 \phi_i = \varphi_i$, is the particular solution for φ_i. The same procedure for developing the BEM for the Laplace equation is applied on both parts of Eq. (13), producing

$$c_i u_i + \int_\Gamma q^* u d\Gamma - \int_\Gamma u^* q d\Gamma = \sum_{k=1}^{N+L} \alpha_k \left(c_i \phi_{ik} + \int_\Gamma q^* \phi_k d\Gamma - \int_\Gamma u^* \frac{\partial \phi_k}{\partial n} d\Gamma \right) \tag{27}$$

where u_* and q_* are the fundamental solution to the Laplace equation and its normal derivative, respectively. $c_i = \theta/2\pi$is a constant and θ is the internal angle at point x_i in radians. The readers are referred to [30] for more details about the DRM.

We apply the BFM to solve this BIE. After the boundary discretization and the boundary variable approximation, we have the discretized BIE:

$$\begin{aligned} & c_i u_i + \sum_{j=1}^{N} \int_{\Gamma_j} q^*(s,x_i) \sum_{k=1}^{N} N_k(s) u_k d\Gamma(s) \\ & \quad - \sum_{j=1}^{N} \int_{\Gamma_j} u^*(s,x_i) \sum_{k=1}^{N} N_k(\mathbf{s}) q_k d\Gamma(s) \\ & = \sum_{m=1}^{N+L} \alpha_m \left(c_i \phi_{im} + \sum_{j=1}^{N} \int_{\Gamma_j} q^*(s,x_i) \sum_{k=1}^{N} N_k(s) \phi_{km} d\Gamma(s) \right. \\ & \quad \left. - \sum_{j=1}^{N} \int_{\Gamma_j} u^*(s,x_i) \sum_{k=1}^{N} N_k(s) \hat{q}_{km} d\Gamma(s) \right) \end{aligned} \tag{28}$$

where $\phi_{km} = \phi_m(x_k)$ and $q_{km} = \partial \phi_m / \partial n(x_k)$. The boundary variable approximation is performed in the parametric spaces. It is of the form:

$$\begin{aligned} u(x,y,z) &= u(u,v) = u(\xi,\eta) = \sum_{k=1}^{N} N_k(\xi,\eta) u_k \\ q(x,y,z) &= u(u,v) = u(\xi,\eta) = \sum_{k=1}^{N} N_k(\xi,\eta) q_k \end{aligned} \tag{29}$$

where (u,v) is the parametric coordinate of (x,y,z) on the surface, and (ξ,η) is the corresponding normalized parametric coordinate.

The matrix form of Eq. (28) is given by

$$H\mathbf{u} - G\mathbf{q} = (H\hat{U} - G\hat{Q})\alpha \tag{30}$$

in which $\hat{U}_{ij} = \phi_{ij}, \hat{Q}_{ij} = \hat{q}_{ij}$.

After the system above is solved, the potential at any internal location can be calculated from equation:

$$u_i = -\sum_{k=1}^{N} H_{ik} u_k + \sum_{k=1}^{N} G_{ik} q_k + \sum_{j=1}^{N+L} \alpha_i \left(\hat{\phi}_{ij} + \sum_{k=1}^{N} H_{ik} \hat{\phi}_{kj} - \sum_{k=1}^{N} G_{ik} \hat{q}_{kj} \right) \tag{31}$$

where

$$H_{ik} = \sum_{j=1}^{N} \int_{\Gamma_j} q^*(s,x_i) N_k(s) d\Gamma(s)$$

and

$$G_{ik} = \sum_{j=1}^{N} \int_{\Gamma_j} u^*(s,x_i) N_k(s) d\Gamma(s)$$

In the DRBFM, much time is consumed to calculate the inversed RBF interpolation matrix, and the solution of Eqs. (30) also poses high computational cost.

4.2. Illustrative numerical examples

The DRBFM equipped with variable shaped RBF has been tested for three types of 3-D geometrical objects: a cube, a sphere and an elbow pipe. The first model is taken to compare the variable shaped RBF with the constant shaped RBF in DRBFM. The following model is taken to compare the numerical solution of a BVP on a torus by DRBFM with the analytical solution. The third model is taken to show the convergence of our method.

In all examples, the variables on each face are interpolated by discontinuous quadric surface elements (parametric formed) with 9 interpolating nodes, and the variable shaped MQ is implemented with its variation scheme,$c_i = h_i^2$, as we proposed in Section 3.

For the purpose of error estimation and convergence study, a 'global' L_2 norm error, normalized by $|v|_{\max}$, is defined as follows [22]:

$$e = \frac{1}{|v|_{\max}} \sqrt{\frac{1}{N} \sum_{i=1}^{N} (v_i^{(e)} - v_i^{(n)})^2} \tag{32}$$

where $|v|_{\max}$ is the maximum value of u or q over N sample points, and the superscripts (e) and (n) refer to the exact and numerical solutions, respectively.

4.2.1. Dirichlet BVP on a cube

$$\begin{cases} \nabla^2 u = -50\cos(3x)\sin(4y)\sin(5z) + 6 & (x,y,z) \in \Omega \\ u = \cos(3x)\sin(4y)\sin(5z) + x^2 + 2y^2 + 3z + 1 & (x,y,z) \in \Gamma \end{cases}$$

where

$$\Omega = \{(x,y,z) | -0.5 < x < 0.5, -0.5 < y < 0.5, -0.5 < z < 0.5\}$$

The exact solution of this problem is

$$u=\cos(3x)\sin(4y)\sin(5z)+x^2+2y^2+3z+1$$

Both the constant shaped RBF and the variable shaped RBF are applied in this example. The constant shape parameter was chosen as 1.5, as proposed by Wang and Liu [31] in 2D interpolation. In the procedure, more interpolation points are distributed near the boundary to improve the interpolation accuracy near the boundary.

The convergence of the interpolation using constant RBF was guaranteed theoretically. The decrease in error of RBF interpolation in this example is shown in Table 1. From Fig. 7, however, we can see that the DRBFM using constant shape RBF numerically diverges. In the other hand, although the convergence and the stability of the present interpolation method have not been testified up to now, and the errors are two or three orders of magnitude more than that of the constant shape RBF interpolation (see Table 1), the error of DRBFM using variable shaped RBF goes to zero stably (see Fig. 7). The reason for this can be found in Fig. 8, which shows the condition number of the interpolation matrix appears in both cases. From Fig. 8, we can see that constant shaped RBF results in ill conditioned matrix, and the result of the DRBFM breaks down when the condition number of the RBF interpolation matrix exceeds 10^{16}. This example clearly demonstrates that the stability of the RBF interpolation is an important factor that affects the accuracy of the DRBFM, and that using variable shaped MQ with the variation scheme$c_i=h_i^2$, the DRBFM is reliable.

Moreover, another observation can be made in Table 1. Accurate interpolation results of the constant shaped RBF can be also obtained even when the condition number exceeds 10^{16}. As pointed out in [29], this can be explained by the "effective condition number", which was proposed by Chan and Foulser [32]. Li and Huang [33] have found that the effective condition number can be smaller than the traditional one by a few orders, and they investigated the effective condition number for numerical partial differential equation.

Table 1
Comparisons of accuracy of the RBFs using constant and variable shape parameters.

Number of interpolation points	Error of constant shape RBF (%)	Error of variable shape RBF (%)
544	0.001520	0.2764
952	0.0003302	0.2165
2856	0.001080	0.1297
4200	0.001590	0.03081

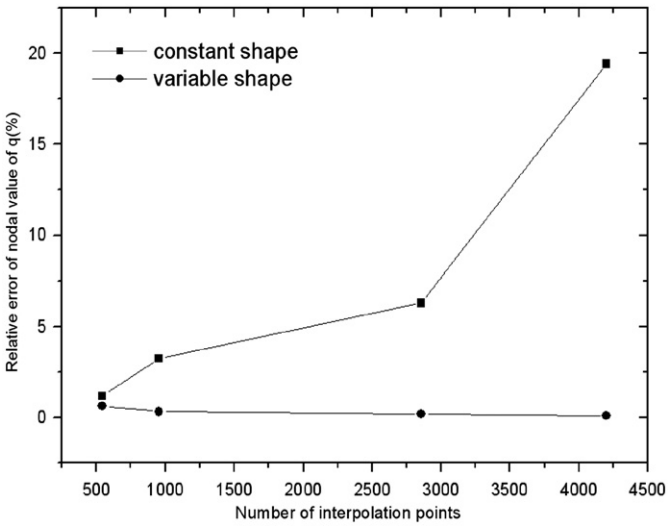

Fig. 7. Comparison of the convergence of the DRBFM between constant case and variation case.

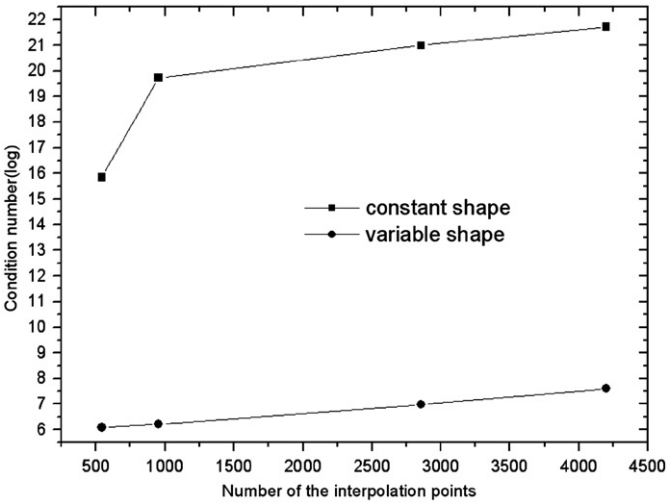

Fig. 8. Comparison of the stability of the DRBFM between constant case and variation case.

4.2.2. Dirichlet problems on a domain bounded by a torus

This example considers a problem in a torus centered at the origin; the exterior radius and the interior radius of the torus are 2 and 0.5 units, respectively (see Fig. 9). This example is presented here to verify the accuracy of the DRBFM. The analytical result is given by

$$u=\cos(x)\sin(1.2y)\sin(1.5z)+x^2+2y^2+2x+2.5y+3z+1$$

The results are obtained using 77 surface elements and 1050 interpolation points (see Fig. 9).

Figs. 10 and 11 show variation in the potential and its directional derivative at locations inside the torus. The gradient is dotted with the direction (1, 0, 0) in order to get the directional derivative along this direction. The sample points are given by

$$\left\{P_i=(x_i,y_i,z_i)|z_i=0,\ x_i=2\cos\varphi_i,\ y_i=2\sin\varphi_i,\ \varphi_i=\frac{(i-1)}{6}\pi,\ i=1,2,\ldots,12\right\}$$

It is seen that the numerical results are in good agreement with the analytical solutions both on potential and flux. It demonstrates that the DRBFM equipped with variable shaped MQ is very efficient.

4.2.3. BVPs with mixed boundary on a sphere

In order to further demonstrate the convergence of the DRBFM, the case of the field for a sphere domain governed by three Poisson equations is presented as the last example. The sphere with a radius of 2 units is centered at the origin. The essential boundary conditions are imposed on half part of the sphere denoted by Γ_1, and the nature boundary conditions are imposed on the other part denoted by Γ_2. The three BVPs are listed as follows:

Problem 1:

$$\begin{cases}\nabla^2 u=12x^2+12xy+6y+14 & (x,y,z)\in\Omega\\ u=x^4+2x^3y+y^3+7z^2+5yz+3z+1 & (x,y,z)\in\Gamma_1\\ \dfrac{\partial u}{\partial n}=2x^4+4x^3y+1.5y^3+5yz+7z^2+1.5z & (x,y,z)\in\Gamma_2\end{cases}$$

with its exact solution:

$$u=x^4+2x^3y+y^3+7z^2+5yz+3z+1.$$

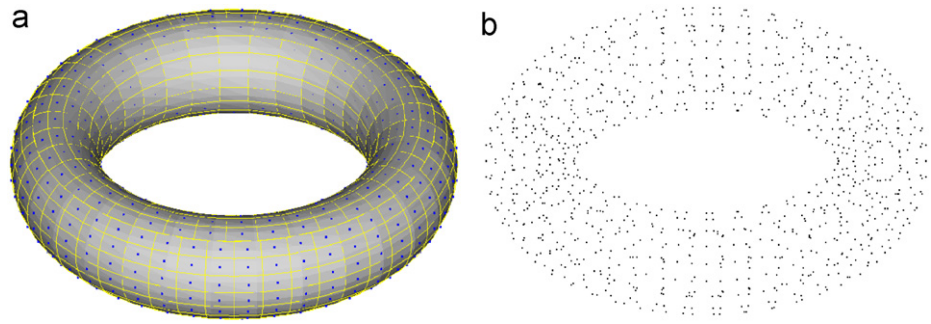

Fig. 9. 77 surface elements (702 nodes) and 1050 RBF centers.

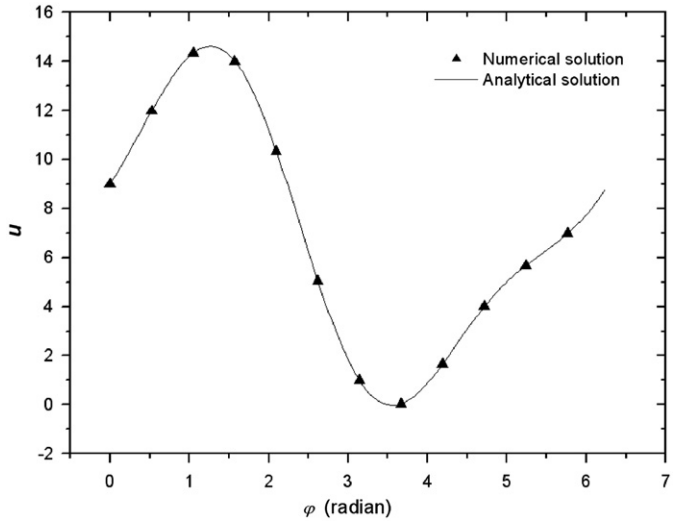

Fig. 10. Variation in potential u along the central circle.

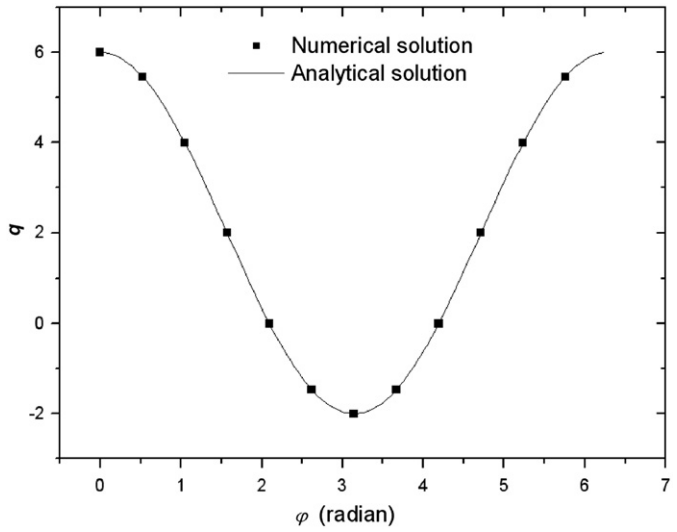

Fig. 11. Variation in flux q along the direction (1, 0, 0).

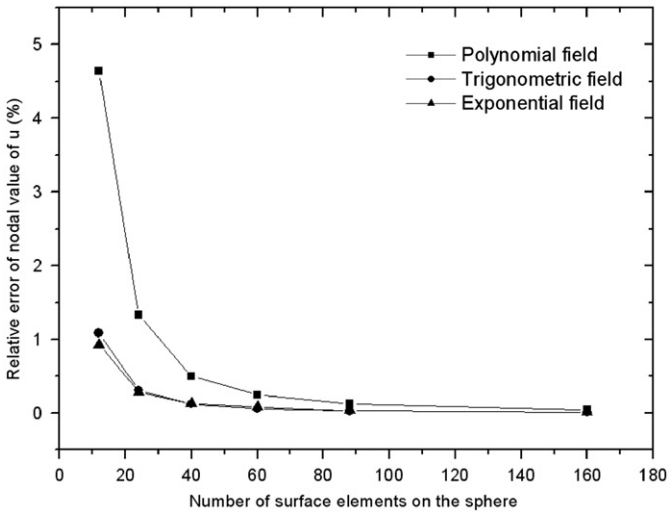

Fig. 12. Variation in L_2 error of u for different number of surface elements on surface.

Problem 2:

$$\begin{cases} \nabla^2 u = -6.93\sin(1.2x)\sin(1.5y)\sin(1.8z)+4 & (x,y,z)\in\Omega \\ u = \sin(1.2x)\sin(1.5y)\sin(1.8z)+2x^2+6y+1 & (x,y,z)\in\Gamma_1 \\ \dfrac{\partial u}{\partial n} = 0.6x\cos(1.2x)\sin(1.5y)\sin(1.8z)+2x^2+0.75y\sin(1.2x)\cos(1.5y)\sin(1.8z) & (x,y,z)\in\Gamma_2 \\ \quad +3y+0.9z\sin(1.2x)\sin(1.5y)\cos(1.8z) \end{cases}$$

with its exact solution:

$$u = \sin(1.2x)\sin(1.5y)\sin(1.8z)+2x^2+6y+1$$

Problem 3:

$$\begin{cases} \nabla^2 u = e^x+1.21e^{1.1y}+1.44e^{1.2z} & (x,y,z)\in\Omega \\ u = e^x+e^{1.1y}+e^{1.2z} & (x,y,z)\in\Gamma_1 \\ \dfrac{\partial u}{\partial n} = 0.5xe^x+0.55ye^{1.1y}+0.6ze^{1.2z} & (x,y,z)\in\Gamma_2 \end{cases}$$

with its exact solution:

$$u = e^x+e^{1.1y}+e^{1.2z}$$

L_2 errors of nodal values of u and $q=\partial u/\partial n$ are shown in Figs. 12 and 13, respectively. We can see that more accurate nodal values can be obtained using more surface elements in three problems. This example shows the convergence of our method. It is worth noting that the result of the polynomial case is not agreeing well in comparison with other two cases. This can be caused by the interpolated function $f=12x^2+12xy+6y+14$, which varies rapidly in the consider domain. The function with a steep

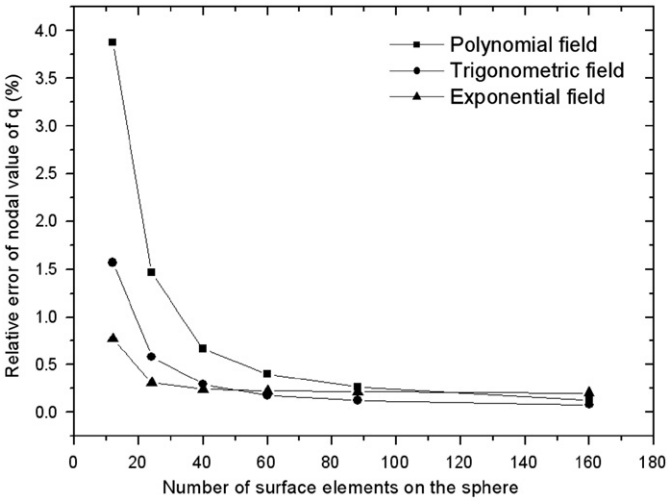

Fig. 13. Variation in L_2 error of q for different number of surface elements on surface.

gradient is usually difficult to be interpolated by the MQ whose gradient is much flatter.

5. Conclusions and future work

We have proposed several shape parameter variation schemes for the variable shaped RBF in order to improve the stability of the interpolation. It has been demonstrated that a better conditioned interpolation matrix can be obtained using the variable shaped RBF with the proposed scheme. The convergence of the interpolation using the variable shaped RBF with the proposed scheme has been also verified.

The DRM and the BFM are combined for solving Poisson equations. A number of numerical examples with different geometries, different boundary condition types and different known analytical solutions are presented. Results demonstrate the high accuracy of our method and that the RBFs with variable shape parameters outperform that with constant parameters.

The BFM needs only boundary discretization in the parametric space of the surface of a body, and the DRM requires only internal points rather than grids. The DRBFM has real potential to seamlessly interact with CAD software to handle arbitrary trimmed solids and to solve practical engineering problems. By coupling with the FMM [34–36], the DRBFM may be able to perform large-scale computations for complicated structures, which is an ongoing work of our research. Developing a fast algorithm for calculating the near singular integrals appeared in the BFM is also ongoing.

Acknowledgements

This work was supported in part by National Science Foundation of China under grant number 10972074, in part by National 863 Program of China under grant number 2008AA042507 and in part by National 973 Project of China under grant number 2010CB328005.

References

[1] Nardini D, Brebbia CA. A new approach to free vibration analysis using boundary elements. Boundary Element Methods in Engineering. Berlin and New York: Computational Mechanics Publications, Southampton and Springer-Verlag; 1982.
[2] Chen JT, Chang MH, Chen KH, Lin SR. The boundary collocation method with meshless concept for acoustic eigenanalysis of two-dimensional cavities using radial basis function. J Sound Vib 2002;4:667–711.
[3] Chen JT, Chen. IL, Chen KH, Yeh YT, Lee YT. A meshless method for free vibration of arbitrarily shaped plates with clamped boundaries using radial basis function. Eng Anal Bound Elem 2004;5:535–45.
[4] Schaback R. Error estimates and condition numbers for radial basis function interpolation. Adv Comput Math 1995;3:251–64.
[5] Yoon J. Interpolation by radial basis functions on Sobolev space. J Approx Theory 2001;11:1–15.
[6] Narcowich FJ, Ward JD, Wendland H. Refined error estimates for radial basis function interpolation. Constr Approx 2003;19:541–64.
[7] Brownlee RA. Error estimates for interpolation of rough data using the scattered shifts of a radial basis function. Numer Algorithms 2005;39: 57–68.
[8] Wendland H. Error estimates for interpolation by radial basis functions of minimal degree. J Approx Theory 1998;93:258–72.
[9] Kansa EJ, Hon YC. Circumventing the ill-conditioning problem with multiquadric radial basis functions: applications to elliptic partial differential equations. Comput Math Appl 2000;39:123–37.
[10] Kansa EJ, Carlson RE. Improved accuracy of multiquadric interpolation using variable shape parameters. Comput Math Appl 1992;24:99–120.
[11] Fornberg B, Zuev J. The runge phenomenon and spatially variable shape parameters in RBF interpolation. Comput Math Appl 2007;54:379–98.
[12] Bozzini M, Lenarduzzi L, Rossini M, Schaback R. Interpolation by basis functions of different scales and shapes. Calcolo 2004;41:77–87.
[13] Sarra SA, Sturgill D. A random variable shape parameter strategy for radial basis function approximation methods. Eng Anal Bound Elem 2009;33: 1239–45.
[14] Li X, Zhu J, Zhang S. A hybrid radial boundary node method based on radial basis point interpolation. Eng Anal Bound Elem 2009;33:1273–83.
[15] Goldberg MA, Chen CS, Bowman H, Power H. Some comments on the use of radial basis functions in the dual reciprocity method. Comput Mech 1998;21:141–8.
[16] Zhang JM, Qin XY, Han X, Li GY. A boundary face method for potential problems in three dimensions. Int J Numer Meth Eng 2009;80:320–37.
[17] Zhang JM, Yao ZH, Li H. A hybrid boundary node method. Int J Numer Meth Eng 2002;53:751–63.
[18] Zhang JM, Yao ZH. Meshless regular hybrid boundary node method. Comput Model Eng Sci 2001;2:307–18.
[19] Zhang JM, Yao ZH, Tanaka M. The meshless regular hybrid boundary node method for 2-D linear elasticity. Eng Anal Bound Elem 2003;27: 259–68.
[20] Zhang JM, Yao ZH. Analysis of 2-D thin structures by the meshless regular hybrid boundary node method. Acta Mech Solida Sinica 2002;15:36–44.
[21] Mukherjee YX, Mukherjee S. The boundary node method for potential problems. Int J Numer Meth Eng 1997;40:797–815.
[22] Chati MK, Mukherjee S. The boundary node method for three-dimensional problems in potential theory. Int J Numer Meth Eng 2000;47:1523–47.
[23] Qin XY, Zhang JM, Li GY, Sheng XM, Song Q, Mu DH. A finite element implementation of the boundary face method for potential problems in three dimensions. Eng Anal Bound Elem 2010;34:934–43.
[24] Chen W, Tanaka M. A meshless, exponential convergence, integration-free, and boundary-only RBF technique. Comput Math Appl 2002;43:379–91.
[25] Fu Z, Chen W, Yang W. Winkler plate bending problems by a truly boundary-only boundary particle method. Comput Mech 2009;44:757–63.
[26] Wu ZM. Multivariate compactly supported positive definite radial functions. Adv Comput Math 1995;4:283–92.
[27] Wendland H. Piecewise polynomial, positive definite and compactly supported radial functions of minimal degree. Adv Comput Math 1995;4:389–96.
[28] Buhmann MD. A new class of radial basis functions with compact support. Math Comput 2000;70:307–18.
[29] Huang CS, Lee CF, Cheng AHD. Error estimate, optimal shape factor, and high precision computation of multiquadric collocation method. Eng Anal Bound Elem 2007;31:614–23.
[30] Partridge PW, Brebbia CA, Wrobel LC. The Dual Reciprocity Boundary Element Method. Berlin and New York: Computational Mechanics Publications, Southampton and Springer-Verlag; 1992.
[31] Wang JG, Liu GR. On the optimal shape parameters of radial basis functions used for 2-D meshless method. Comput Methods Appl Mech Eng 2002;191:2611–30.
[32] Chan TF, Foulser DE. Effectively well-conditioned linear systems. SIAM J Sci Stat Comput 1988;9:963–9.
[33] Li ZC, Huang HT. Effective condition number for numerical partial differential equations. Numer Linear Algebra Appl 2008;7:575–94.
[34] Zhang JM, Tanaka M, Endo M. The hybrid boundary node method accelerated by fast multipole method for 3D potential problems. Int J Numer Meth Eng 2005;63:660–80.
[35] Zhang JM, Tanaka M. Fast HdBNM for large-scale thermal analysis of CNT-reinforced composites. Comput Mech 2008;41:777–87.
[36] Zhang JM, Tanaka M. Adaptive spatial decomposition in fast multipole method. J Comput Phys 2007;226:17–28.